Experimental Impacts into Strength-Layered Targets: Ejecta Kinematics. J.L.B. Anderson[1], M.J. Cintala[2], C.J. Cline II[3], L.E. Dechant[1], J.M. Ebel[1], R.A. Taitano[1], and J.B. Plescia[4]. [1]Geoscience, Winona State Univ., Winona, MN 55987. [2]Code X13, NASA Johnson Space Center, Houston, TX 77058. [3]Jacobs, NASA Johnson Space Center, Houston, TX 77058. [4]Applied Physics Lab, Johns Hopkins Univ., Laurel, MD 20723. (Contact: JLAnderson@winona.edu)

Introduction: Impact cratering has dominated the evolution and modification of planetary surfaces throughout the history of the solar system. Impact craters can serve as probes to understanding the details of a planetary subsurface; for example, Oberbeck and Quaide [1-2], suggested that crater morphology can be used to estimate the thickness of a regolith layer on top of a more competent unit. Lunar craters show a morphological progression from a simple bowl shape to flat-floored and concentric craters as crater diameter increases for a given regolith thickness.

The final shape of the impact crater is a result of the subsurface flow-field initiated as the projectile transfers its energy and momentum to the target surface at the moment of impact. Therefore, when a regolith layer is present over a stronger substrate, such as is the case on the lunar surface, the substrate modifies the flow-field and thereby the excavation flow of the crater, which is reflected in the morphology of the final crater. Here we report on a series of experimental impacts into targets composed of a thin layer of loose sand on top of a stronger substrate. We use the Ejection-Velocity Measurement System (EVMS, Fig. 1) developed by [3] to examine the ejecta kinematics during the formation of these craters.

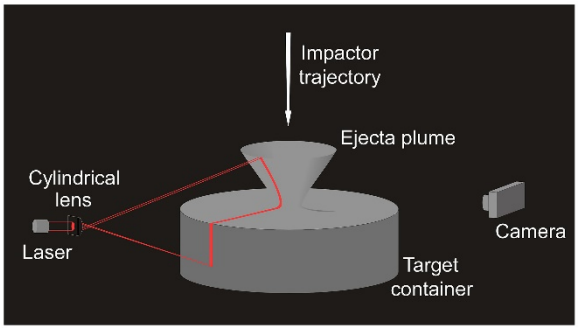

Figure 1. Ejection-Velocity Measurement System (EVMS).

Experiment Design: Experimental impacts were performed in near-vacuum (< 1 torr) with with 4.76-mm aluminum projectiles impacting the target at 1.54 km/s (± 0.02 km/s) and normal to the target surface. A well-sorted quartz sand (0.4-0.8 mm grain size) served as a regolith layer of varying thickness over a stronger substrate made of chemically bonded sand (grain size < 0.5 mm). The thickness of the regolith was varied from 0 to 5 cm. These impacts were compared to a control experiment that used a 12-cm deep target of the unbonded 0.4-0.8 mm sand [4].

The EVMS projects a vertical laser sheet perpendicular to the target surface and passing through the impact point, thus illuminating a vertical slice of the advancing ejecta curtain (Fig. 1). This laser is strobed at a pre-defined rate and particles are illuminated multiple times along their ballistic trajectories as imaged by the camera (Fig. 2). The resulting image is digitized and processed to determine ejection position, angle, and speed that can be related through scaling relationships [e.g., 3]. 3D scans were also recorded before and after each experiment, permitting close examination of the final crater morphology and morphometry with respect to the original stratigraphy of the target. (Please see Anderson *et al.*, this conference [5], for our related discussion of crater morphometries observed in these experiments.)

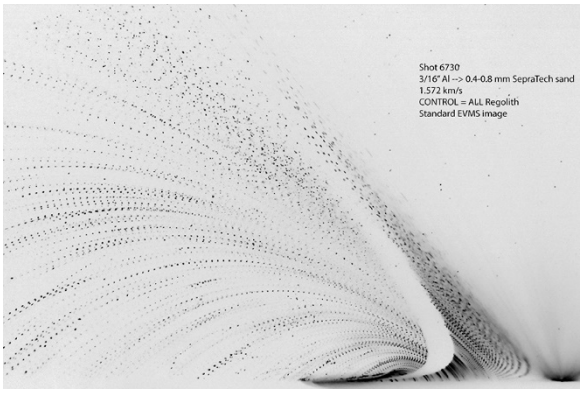

Figure 2. Experimental impact of 4.76-mm Aluminum sphere into a control target composed entirely of loose sand. Note the well-behaved ejecta trajectories.

Initial Results: As expected, the ejecta kinematics of the control target with no stronger substrate at depth was typical (Fig. 2). The addition of the stronger substrate below the regolith layer, however, produced a much more complex pattern of ejecta (Fig. 3). As of this writing, we can make four major observations from the EVMS images obtained during this series of experiments. (1) Much of the ejected material is still part of a typical curtain moving outward with time as the crater is excavated, but (2) there are some interesting "dog-legs" or kinks that appear in the shape of the advancing

ejecta curtain. (3) There are a number of ejected particles that move along low-speed, high-angle trajectories. We had never seen such trajectories in our experiments prior to adding the stronger layer at depth. (4) The relative number of these high-angle trajectories increases as the regolith layer thins. It is clear that this excavation-stage flow is a result of the stronger substrate.

Figure 3. EVMS image of target with 2-cm thick sand layer on top of stronger substrate.

Current Work: As a result of this very complicated ejection sequence, we have modified our method of obtaining and analyzing EVMS images. Since the shutter of the EVMS camera is left open for all of crater growth (about 600 msec total) while the laser is strobed, we do not know exactly when during rater excavatin these high-angle ejecta particles appear. Thus, we have completed a second series of impact experiments using only 2-cm thick regolith targets and setting the EVMS to capture the ejecta in 10-20-msec snapshots (Fig. 4) over the entire course of crater growth. We have begun processing these EVMS images and exploring how the ejecta kinematics in the layered targets differ from that of the control experiment (Fig. 5). Should these observations hold up and scale with crater size, these results imply that self-secondary cratering [6] would require the presence of a strong subsurface layer below the impact site.

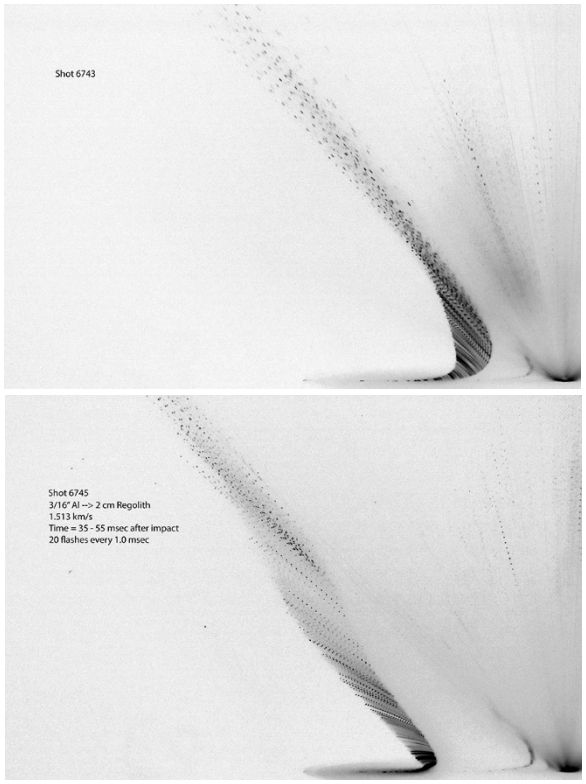

Figure 4. (A) 5-15 msec and (B) 35-55 msec after impact.

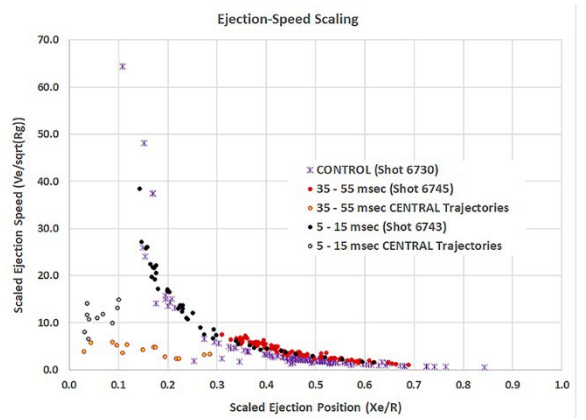

Figure 5. Ejection-speed scaling for ejecta observed during impacts into 2-cm thick regolith targets (Figs. 2 & 4). Note the low-velocity particles that are ejected from very near to the crater center. These particles also have very high ejection angles (> 50°).

Acknowledgements: This work would not have been possible without the EIL gunners Frank Cardenas and Roland Montes as well as Captain Electron, Terry Byers. And many thanks to Luke Zwiefelhofer and Nikki Schossow at Winona State.
This work is supported by NASA SSW grant NNX16AR92G.

References: [1] Oberbeck & Quaide 1967, JGR **72**, 4697-4704. [2] Quaide & Oberbeck 1968, JGR **73**, 5247-5270. [3] Cintala *et al.* 1999, MAPS **34**. [4] Cline *et al.* 2019, **AGU** #3504. [5] Anderson *et al.* 2020, **LPSC**. [6] Plescia & Robinson 2019, Icarus **321**, 974-993.